Orbital and CO_2 forcing of late Paleozoic continental ice sheets

Daniel E. Horton,[1] Christopher J. Poulsen,[1] and David Pollard[2]

Received 30 June 2007; revised 28 August 2007; accepted 30 August 2007; published 11 October 2007.

[1] Contrasting views of the size, duration, and history of the Gondwanan continental ice sheets have been proposed from late Paleozoic glaciological and sedimentological evidence. To evaluate these differing views, a coupled ice sheet-climate model is used to simulate continental ice sheets under a wide range of late Paleozoic orbital and pCO_2 conditions. The model experiments indicate that orbital variations at pCO_2 concentrations below 2X pre-industrial atmospheric levels (PAL; 280 ppm) produce large changes in late Paleozoic ice volume ($\sim 1.3 \times 10^8$ km^3) and sea level ($\sim$20 to 245 m). Between 2 and 8X PAL Gondwana continental ice is simulated only under the most extreme Southern Hemisphere cold summer orbit, but still produces significant ice volumes ($\sim 8-12 \times 10^7$ km^3). Our results highlight the important role of atmospheric CO_2 in determining the distribution, volume, and stability of late Paleozoic ice sheets, factors that ultimately impacted sea level, cyclothem deposition, and global climate, and reconcile disparate views of the Late Paleozoic Ice Age.
Citation: Horton, D. E., C. J. Poulsen, and D. Pollard (2007), Orbital and CO_2 forcing of late Paleozoic continental ice sheets, *Geophys. Res. Lett.*, *34*, L19708, doi:10.1029/2007GL031188.

1. Introduction

[2] The late Paleozoic ice age (LPIA) was the most severe glaciation in the Phanerozoic, spanning 60 million years (326–267 Ma; *Frakes et al.* [1992]) with peak ice volumes as great or greater than that during the Last Glacial Maximum [*Crowley and Baum*, 1991]. The LPIA has long been considered a single uninterrupted glaciation [*Frakes and Francis*, 1988; *Crowell*, 1978, 1999; *Veevers and Powell*, 1987; *Veevers et al.*, 1994] during which ice volume was modulated by insolation variations arising from changes in Earth's orbit [*Heckel*, 1990]. Cyclothems, repetitive successions of marine and non-marine sediments, are often considered to be the stratigraphic signature of orbitally-controlled ice volume fluctuations. Euramerican cyclothems, deposited between the late Namurian (326 Ma) and early Kazanian (260 Ma), are estimated to represent 100 to 230 m of sea-level change [*Crowell*, 1999].

[3] Recent reevaluations of the Gondwana glacial record challenge this view of large orbitally-driven ice volume variations superimposed on a long lived continental glaciation [*Isbell et al.*, 2003a, 2003b; *Fielding et al.*, 2006]. Rather, *Isbell et al.* [2003b] propose that the LPIA consisted of three distinct glacial events (Glacial I, $\sim$375–350 Ma; Glacial II, $\sim$315–307 Ma; and Glacial III, $\sim$299–276 Ma). Continental glaciation was only widespread, covering much of southern Gondwana, during the final event. The complete ablation of the Glacial III ice sheets is estimated to have raised sea-level by only 50 to 115 m, depending on whether continental ice was distributed in multiple ice sheets with small aspect ratios or a single enormous ice dome [*Isbell et al.*, 2003b], an amount that is too small to have generated the accommodation space required for cyclothem deposition.

[4] The cause of the LPIA is not certain, but was likely related to low atmospheric pCO_2 levels. According to the CO_2 proxy record of the last 500 million years, only the Neogene had lower pCO_2 levels [*Royer*, 2006; *Berner and Kothavala*, 2001]. Atmospheric pCO_2 may also have been variable; *Montañez et al.* [2007] report late Carboniferous-middle Permian values that oscillate between $\sim$1 and 8X PAL, with low values coincident with the deposition of glaciogenic sediments on Gondwana.

[5] Two-dimensional energy balance models (EBMs), deriving their ice estimates from summer land temperatures, have been used to investigate the possible size, sensitivities, and location of the late Paleozoic ice age [*Crowley*, 1994]. These models indicate that Gondwana ice sheets could have reached a size similar to that of the Pleistocene glaciation [*Crowley and Baum*, 1991] and predict sea-level changes of 70 to 100 m [*Crowley and Baum*, 1992]. Additionally, EBMs utilizing prescribed modern Northern Hemisphere precipitation rates (modified by the Clausius-Clapeyron relation) indicate that Permo-Carboniferous ice sheets were likely sensitive to past CO_2 levels, and suggest that past changes in CO_2 are required to explain the onset and demise of continental ice sheets [*Hyde et al.*, 1999; *Hyde et al.*, 2006]. Atmospheric general circulation models (AGCMs) have been used to investigate the global climate response to the glaciation of Gondwana [*Poulsen et al.*, 2007], but to our knowledge have not been used to predict past continental ice sheets.

[6] The goal of this study is to quantify late Paleozoic ice volumes and equivalent sea level under a broad range of likely orbital and pCO_2 values. In contrast to previous studies, we employ an AGCM (with full hydrological cycle) coupled to a 3-D ice-sheet model. Our results provide a framework for interpreting the variability in ice sheets and sea level inferred from the geological record, and help reconcile disparate views of the late Paleozoic ice age.

2. Model and Methods

[7] Late Paleozoic experiments were completed using the GENESIS AGCM version 2.3 coupled to a 3-D dynamic ice sheet model. GENESIS consists of an AGCM coupled to a land-surface model with multi-layer models of vegetation,

[1]Department of Geological Sciences, University of Michigan, Ann Arbor, Michigan, USA.
[2]Earth and Environment Science Institute, Pennsylvania State University, University Park, Pennsylvania, USA.

0094-8276/07/2007GL031188

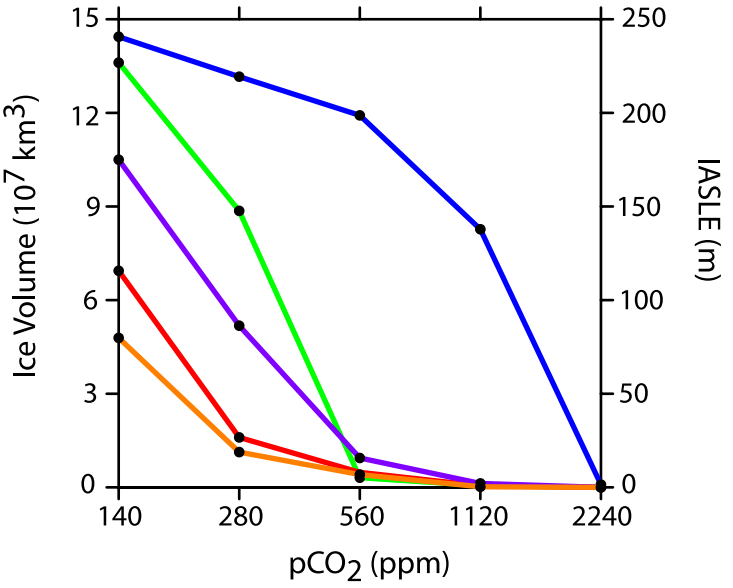

Orbit Description	Abbreviation	Obliquity	Eccentricity	Precession
S.H. Warm Summer	SHWS	24.5	0.06	90
N.H.Cold Summer	NHCS	22.0	0.06	90
Middle Summer	MDS	23.5	0.0	180
N.H. Warm Summer	NHWS	24.5	0.06	270
S.H. Cold Summer	SHCS	22.0	0.06	270

Figure 1. Simulated continental ice volume (10^7 km^3) and isostatically adjusted sea-level equivalent (IASLE) (m) under varying pCO_2 levels and orbital configurations. The filled circles represent the results from each equilibrium experiment. The various lines connect experiments with the same orbital configuration.

soil or land ice, and snow. The AGCM has a spectral resolution of T31 (3.75° × 3.75°), and 18 vertical levels. The land-surface grid has a resolution of 2 × 2°. Sea-surface temperatures and sea ice are computed using a 50-m slab oceanic layer with diffusive heat flux [*Pollard and Thompson*, 1995; *Thompson and Pollard*, 1997].

[8] The 3-D ice sheet model operates on a 1 × 2° surface grid [*Deconto and Pollard*, 2003]. The thermo-mechanical ice-sheet model is based on the vertically integrated continuity equation for ice mass [*Huybrechts*, 1993; *Ritz et al.*, 1997]. The evolution of ice geometry is determined by surface mass balance, basal melting, and ice flow. Ice temperatures are predicted to account for their effect on rheology and basal sliding. The local bedrock response to ice load is a simple relaxation toward isostacy with a time constant of 5,000 years. Lithospheric flexure is modeled by linear elastic deformation. In this version of the model, ice shelves are not simulated.

[9] To couple the climate and ice-sheet models, we use an asynchronous technique that consists of alternating AGCM and ice sheet integrations. To begin, GENESIS is integrated for 30 yrs to produce a steady-state climatology. Mean monthly meteorological fields (i.e. surface air temperature, evaporation, and precipitation) from the last ten years drive the ice-sheet model. Each ice-sheet model experiment is run for 200,000 yrs, though ice-sheet equilibria are typically reached after 50,000 yrs, and predicts ice-sheet area, thickness, and isostatically adjusted continental topography. These boundary conditions are incorporated into the AGCM, which is run for an additional 20 yrs. Meteorological fields from the last ten years of this AGCM iteration drive a final 200,000 yr iteration of the ice-sheet model. In our experience, two climate-ice sheet iterations are sufficient to bring the system into equilibrium; additional iterations have little effect on the climate and ice-sheet solutions.

[10] In total, twenty-five Sakmarian (281 Ma) experiments were carried out with different atmospheric pCO_2 and orbital parameters. Experiments were developed for five different atmospheric pCO_2 levels: 0.5 (140 ppm), 1 (280 ppm), 2 (560 ppm), 4 (1120 ppm) and 8 (2240 ppm) × PAL. These values span the range reported by *Montañez et al.* [2007] for the Permo-Carboniferous. At each pCO_2 level five experiments were developed with different orbital settings (Figure 1). The range of orbital settings used in these experiments is based on the solar calculations of *Berger and Loutre* [1991] for the last ten million years and represent seasonal insolation extremes.

[11] All other boundary conditions are identical between experiments, and were chosen where possible to represent Sakmarian conditions. The paleogeography and paleotopography are based on the Paleogeographic Atlas Project's reconstruction for this time interval [*Ziegler et al.*, 1997]. Because our objective is to estimate continental ice, we modified the Sakmarian paleogeography by removing any prescribed continental ice. The ocean diffusive heat flux was set to a value that provides the best simulation for the modern climate. The late Paleozoic solar luminosity was specified as 1330.3 Wm^{-2}, 3% less than modern, in accordance with solar evolution models [*Gough*, 1981]. In

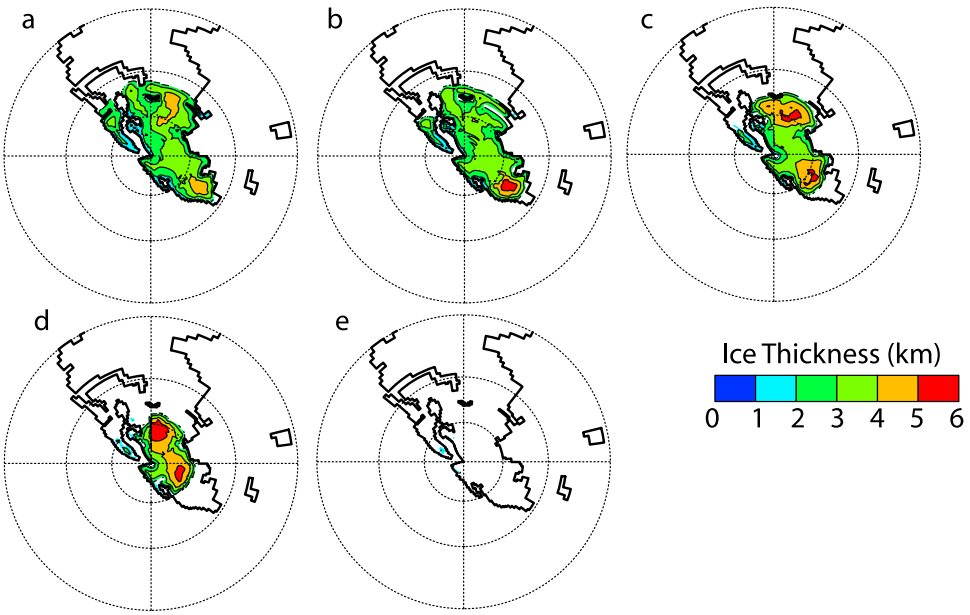

Figure 2. Southern Hemisphere continental ice thickness (m) response to atmospheric pCO_2. The orbital configuration (SHCS) is identical in all experiments. The pCO_2 concentration is (a) 140, (b) 280, (c) 560, (d) 1120, and (e) 2240 ppm. The dashed line in the polar projection map shows the paleolatitude with a contour interval of 30°.

the absence of proxy estimates for the late Paleozoic, trace gas concentrations of CH_4 (0.650 ppm) and N_2O (0.285 ppm) were set to pre-industrial levels.

[12] To estimate the sea-level change represented by our ice volume simulations, we employ the methods of *Crowley and Baum* [1991] and *Paterson* [1994]. The simulated global ice volume in each experiment is converted to a water equivalent (WE) assuming an ice density of 0.917 g/mL. We then estimate an isostatically adjusted sea-level equivalent (IASLE) by:

$$\text{IASLE} = (1 - k) \times \text{WE/ocean surface area}$$

where k has a value of 0.284 (the ratio of seawater density to oceanic lithosphere density). The isostatic adjustment approximates the response of the oceanic lithosphere to seawater loading/unloading. The Permian ocean surface area (386.4×10^6 km^2) was calculated from the Sakmarian paleogeographic reconstruction.

3. Results

3.1. CO_2 Sensitivity

[13] Our experiments indicate that Gondwana ice volume varies significantly with atmospheric pCO_2 (Figures 1 and 2). Under all orbital conditions, significant ice is simulated at pCO_2 levels below 2X PAL. At levels of 8X PAL or higher, no continental ice is simulated even in the most favorable orbit (Figure 1). In our simulations, pCO_2 controls ice volume through its influence on high-latitude surface temperature (Figure 3a). Significant ice volumes are simulated when high-latitude surface temperatures remain below freezing through the year. At pCO_2 levels greater than 2X PAL, when surface temperatures exceed the melting point of ice, continental ice disappears (for example, compare Figures 1 and 3a for NHWS case (green line)). The CO_2-ice volume relationship becomes highly non-linear as temperatures exceed the freezing point because the average annual ablation rate (~0.5 to 1.0 m°C^{-1}) is an order of magnitude greater than variations in annual snowfall.

[14] The distribution of continental ice on Gondwana is also sensitive to atmospheric pCO_2. In all simulations, continental ice is distributed among multiple sheets on Gondwana, including south-central Africa and southern Australia, consistent with glacio-sedimentological reconstructions [*Fielding et al.*, 2006]. The location of the principal ice spreading centers coincides with those areas whose basal temperatures are sufficient to freeze the ice sheet to the surface and prohibit basal sliding. At low pCO_2, continental ice sheets are widespread, reaching nearly 35°S, but are relatively thin. At higher pCO_2, continental ice extends to only 52°S, but is concentrated in two ice sheets with heights over 5 km (Figure 2). This variation in ice-sheet thickness at different CO_2 concentrations is controlled by differences in precipitation over Gondwana. The temperature increase induced by higher greenhouse gas concentrations leads to a higher saturation vapor pressure, resulting in greater atmospheric water vapor, and ultimately greater precipitation. The increase in precipitable snow accumulation (up to ~20 cm yr^{-1}) at higher CO_2 levels results in greater ice sheet dome height. In these experiments, there is no direct relationship between the Sakmarian paleotopography and the spreading center locations.

3.2. Orbital Sensitivity

[15] Orbital variations have a substantial impact on Pangean ice volume (Figure 1). In the 2X PAL CO_2 experiment, for example, global ice volume varies from 4.19×10^6 km^3 with a SHWS orbit to 1.19×10^8 km^3 with a SHCS orbit. These differences in global ice volume mainly reflect

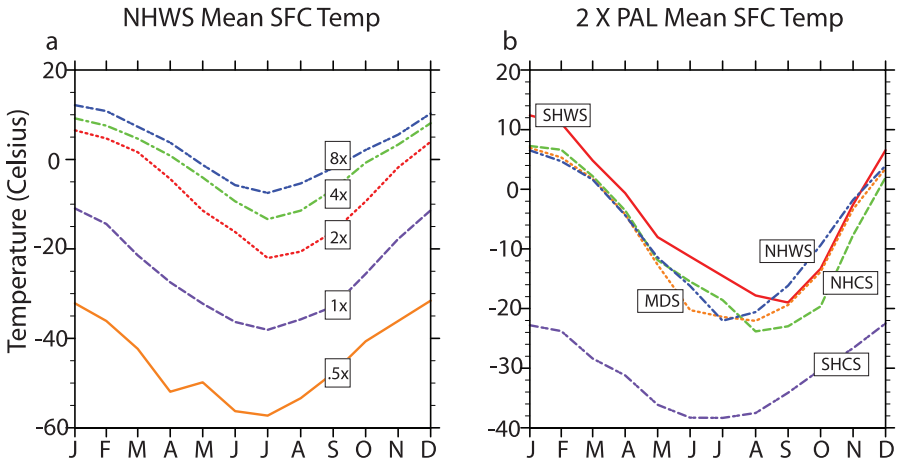

Figure 3. (a) Monthly average surface temperature at 65°S for a range of pCO_2 concentrations during a Northern Hemisphere warm summer orbit (NHWS). (b) Monthly average surface temperature at 65°S at 2X PAL pCO_2 for various orbital configurations.

changes in ice volume over Gondwana and are controlled by high-latitude summer insolation in the Southern Hemisphere, which varies from 520 W/m^2 at 65°S in the SHWS case to 375 W/m^2 in the SHCS case. Such variations in insolation produce marked monthly average surface temperature differences (demonstrated at 65°S in Figure 3b) and help to regulate ice-sheet growth and ablation. In orbits that minimize NH summer insolation a small continental ice sheet develops in northern Pangea, but its volume has a negligible affect on global ice volume.

3.3. Sea-Level Change

[16] Atmospheric pCO_2 concentration and orbital variability have a significant effect on potential sea-level change in the late Paleozoic. The total ablation of simulated continental ice sheets in our experiments represents isostatically-adjusted sea-level changes of up to 245 m (Figure 1). Assuming that Earth's late Paleozoic orbital variability was similar to that of the last 10 million years, our results predict large (~100 m) sea-level changes on 10^4 year timescales at low pCO_2. However, between 2 and 4X PAL, substantial ice develops only at the most extreme orbits. As a result, the frequency of sea-level change would have decreased, operating on 10^5 year timescales (i.e. at times of high eccentricity and low obliquity). Above 4X PAL, large continental ice sheets are not simulated under any orbital condition, eliminating the possibility of significant glacioeustatic change.

4. Caveats

[17] To our knowledge, this study is the first to estimate late Paleozoic continental ice over a large range of orbital and pCO_2 conditions using an AGCM. A number of simplifications and assumptions were made in the development and execution of our experiments. To predict ice volumes under a range of orbital conditions, we have simulated equilibrium ice sheets for specific orbits (see Section 2). In reality, equilibrium conditions were probably never attained since orbital cycles are continuous with periods that are smaller than ice-sheet equilibrium time. As such, the ice volumes attained in our low CO_2/CS (high CO_2/WS) simulations are probably too large (small) because they do not include time-marching orbital configurations. To address this issue we are developing transient simulations with complete orbital cycles.

[18] While the paleogeography of the late Paleozoic is reasonably well understood, the paleotopography is not well constrained. Our simulations of continental ice are likely to be sensitive to continental elevations, since surface temperatures are a function of the environmental lapse rate. For this reason we used a conservative paleotopography with no elevations above 1100 m. Additionally, the model neglects marine ice (grounded below sea level) growing over continental shelves, thus preventing ice formation in embayment areas that could buttress continental ice sheets and produce larger ice volumes.

[19] Another potential limitation is our use of a slab ocean with modern ocean heat fluxes. The specification of a different ocean heat transports has been shown to alter the meridional surface temperature gradient in atmosphere-only GCMs of the Mesozoic [e.g., *Barron et al.*, 1993; *Poulsen et al.*, 1999]. However this strong link between ocean heat transport and meridional temperature gradient does not exist in ocean-atmosphere GCMs [*Poulsen and Huynh*, 2006]. Consequently, it is not clear what effect, if any, the specification of modern ocean heat fluxes has on our simulation of the late Paleozoic ice sheets. We will pursue this issue using a coupled ocean-atmosphere GCM in the future.

5. Discussion and Conclusion

[20] This study provides predictions of late Paleozoic ice-sheet volumes under the influence of varying atmospheric pCO_2 concentrations and orbital parameters. Below 2X PAL, significant Gondwanan ice sheets are simulated for all orbits, though large variations in ice volume exist (Figure 1). Above the 2X PAL threshold large-scale fluctuations in ice-sheet volume can only be expected during a

SHCS orbit (Figure 2). This implies that at pCO_2 values greater than 2X PAL glacial/inter-glacial sequences would occur only at times of maximum eccentricity and minimum obliquity. Above 4X PAL, no significant continental ice is simulated.

[21] The results presented here are broadly consistent with previous late Paleozoic modeling studies [*Crowley and Baum*, 1991; *Hyde et al.*, 1999; *Herrmann et al.*, 2003]. Although our simulations predict multiple domes of ice, our maximum ice volume ($\sim 1.44 \times 10^8$ km^3) is similar to the 1.5×10^8 km^3 reported for the Carboniferous by *Hyde et al.* [1999]. However, our orbital sensitivity experiments indicate that ice volumes of this extent would have endured for no more than $\sim 10^4$ yrs under maximum SHWS insolation values. Our equivalent sea-level change estimates are approximately in line with estimates of 45 to 190 m for the Carboniferous [*Crowley and Baum*, 1991]. Importantly, our IASLE results indicate that the magnitude and frequency of sea-level change would have been very sensitive to the paleo-pCO_2 with maximum sea-level changes of $\sim$200 m at $\sim$560 ppm CO_2.

[22] The variability of ice-sheet volume has profound implications for late Paleozoic sea-level change and cyclothem deposition. Cyclothems have previously been interpreted to represent at least 100 m of sea-level change [*Crowell*, 1999]. Our results indicate that at pCO_2 concentrations at and below 4X PAL, cyclothem deposition would have been possible due to the orbitally driven waxing and waning of continental ice sheets (Figure 1). Above 4X PAL, cyclothem deposition would have ceased due to shrinking ice volumes (Figure 2); a prediction borne out by the disappearance of late Paleozoic cyclothems in the Kazanian [*Crowell*, 1978; *Veevers and Powell*, 1987] and coincident with rising atmospheric pCO_2 [*Montañez et al.*, 2007]. Under these pCO_2-cyclothem thresholds we envision a late Paleozoic with active cyclothem deposition, similar to the glaciation model of *Frakes et al.* [1992] while CO_2 remained at and below 4X PAL. Above 4X PAL, cyclothem deposition could not have been caused by glacioeustasy, consistent with *Isbell et al.* [2003b].

[23] In summary, the results presented here indicate persistent Gondwana glaciation below 2X PAL, and episodic Gondwanan glaciation up to 8X PAL. These theoretical thresholds in conjunction with late Paleozoic proxy CO_2 data indicate that both the icehouse-greenhouse transition of the Permo-Carboniferous and the dynamic nature of orbital scale climate change were most likely the consequence of changes in greenhouse gas concentrations.

[24] **Acknowledgments.** We gratefully acknowledge comments made by H. Hill, W. Hyde, S. Lee, and an anonymous reviewer. This project was supported by grant (0544760) from the National Science Foundation's Sedimentary Geology and Paleontology Program to C. Poulsen.

References

Barron, E. J., W. H. Peterson, D. Pollard, and S. Thompson (1993), Past climate and the role of ocean heat transport: Model simulations for the Cretaceous, *Paleoceanography*, *8*, 785–798.

Berger, A., and M. F. Loutre (1991), Insolation values for the climate of the last 10 million years, *Quat. Sci. Rev.*, *10*(4), 297–317.

Berner, R. A., and Z. Kothavala (2001), GEOCARB III: A revised model of atmospheric CO_2 over Phanerozoic time, *Am. J. Sci.*, *301*, 182–204.

Crowell, J. C. (1978), Gondwana glaciation, cyclothems, continental positioning, and climate change, *Am. J. Sci.*, *278*, 1345–1372.

Crowell, J. C. (1999), Pre-Mesozoic ice ages: Their bearing on understanding the climate system: Boulder, Colorado, *Mem. Geol. Soc. Am.*, *192*, 1–106.

Crowley, T. J. (1994), Pangean climates, in *Pangea: Paleoclimate, Tectonics, and Sedimentation During Accretion, Zenith, and Breakup of a Supercontinent*, edited by G. D. Klein, *Spec. Pap. Geol. Soc. Am.*, *288*, 25–39.

Crowley, T. J., and S. K. Baum (1991), Estimating Carboniferous sea-level fluctuations from Gondwana ice extent, *Geology*, *19*, 975–977.

Crowley, T. J., and S. K. Baum (1992), Modeling late Paleozoic glaciation, *Geology*, *20*, 507–510.

Deconto, R. M., and D. Pollard (2003), A coupled climate-ice sheet modeling approach to the Early Cenzoic history of the Antarctic ice sheet, *Palaeogeogr. Palaeoclimatol. Palaeoecol.*, *198*, 39–52.

Fielding, C. R., K. L. Bann, J. A. Maceachern, S. C. Tyess, and B. G. Jones (2006), Cyclicity in the nearshore marine to coastal, Lower Permian, Pebbly Beach Formation, southern Sydney Basin, Australia: A record of relative sea-level fluctuations at the close of the Late Paleozoic Gondwanan ice age, *Sedimentology*, *53*, 435–463.

Frakes, L. A., and J. E. Francis (1988), A guide to Phanerozoic cold polar climates from high-latitude ice-rafting in the Cretaceous, *Nature*, *333*, 547–549.

Frakes, L. A., J. E. Francis, and J. I. Syktus (1992), *Climate Modes of the Phanerozoic*, 274 pp., Cambridge Univ. Press, Cambridge, U. K.

Gough, D. O. (1981), Solar interior structure and luminosity variations, *Sol. Phys.*, *74*, 21–34.

Heckel, P. H. (1990), Evidence for global (glacial-eustatic) control over upper Carboniferous (Pennsylvanian) cyclothems in mid-continent North America, in *Tectonic Events Responsible for Britain's Oil and Gas Reserves*, edited by R. F. P. Hardman and J. Brooks, *Geol. Soc. Spec. Publ.*, *55*, 35–47.

Herrmann, A. D., M. E. Patzkowsky, and D. Pollard (2003), Obliquity forcing with 8–12 times preindustrial levels of atmospheric pCO_2 during the Late Ordovician glaciation, *Geology*, *31*, 485–488.

Huybrechts, P. (1993), Glaciological modelling of the Late Cenozoic East Antarctic ice sheet: Stability or dynamism?, *Geogr. Ann. Ser. A*, *75*, 221–238.

Hyde, W. T., T. J. Crowley, L. Tarasov, and W. R. Peltier (1999), The Pangean ice age: Studies with a coupled climate-ice sheet model, *Clim. Dyn.*, *15*, 619–629.

Hyde, W. T., E. L. Grossman, T. J. Crowley, D. Pollard, and C. R. Scotese (2006), Siberian glaciation as a constraint on Permian-Carboniferous CO_2 levels, *Geology*, *34*, 421–424.

Isbell, J. L., P. A. Lenaker, R. A. Askin, M. F. Miller, and L. E. Babcock (2003a), Reevaluation of the timing and extent of late Paleozoic glaciation in Gondwana: Role of Transantarctic Mountains, *Geology*, *31*, 977–980.

Isbell, J. L., M. F. Miller, K. L. Wolfe, and P. A. Lenaker (2003b), Timing of late Paleozoic glaciation in Gondwana: Was glaciation responsible for the development of Northern Hemisphere cyclothems?, in *Extreme Depositional Environments: Mega End Members in Geologic Time*, edited by M. A. Chan and A. W. Archer, *Spec. Pap. Geol. Soc. Am.*, *370*, 5–24.

Montañez, I. P., N. J. Tabor, D. Niemeier, W. A. DiMichele, T. D. Frank, C. R. Fielding, J. L. Isbell, L. P. Birgenheier, and M. C. Rygel (2007), CO_2-forced climate and vegetation instability during late Paleozoic deglaciation, *Science*, *315*, 87–91.

Paterson, W. S. B. (1994), *The Physics of Glaciers*, 480 pp., Pergamon, Oxford, U. K.

Pollard, D., and S. L. Thompson (1995), Use of a land-surface-transfer scheme (LSX) in a global climate model (GENESIS): The response to doubling stomatal resistance, *Global Planet. Change*, *10*, 129–161.

Poulsen, C. J., and T. T. Huynh (2006), Paleoceanography of the Mesozoic Pacific: A perspective from climate model simulations, in *Paleogeography of the North American Cordillera: Evidence against Large-Scale Displacements*, edited by J. W. Haggart, R. J. Enkin, and J. W. H. Monger, *Geol. Assoc. Can. Spec. Pap.*, *46*, 13–27.

Poulsen, C. J., E. J. Barron, C. Johnson, and P. Fawcett (1999), Links between major climatic factors and regional oceanic circulation in the mid-Cretaceous, in *Evolution of the Cretaceous Ocean-Climate System*, edited by E. Barrera and C. C. Johnson, *Spec. Pap. Geol. Soc. Am.*, *332*, 73–90.

Poulsen, C. J., D. Pollard, I. P. Montañez, and D. Rowley (2007), Late Paleozoic tropical climate response to Gondwanan deglaciation, *Geology*, *35*, 771–774.

Ritz, C., A. Fabre, and A. Letreguilly (1997), Sensitivity of a Greenland ice sheet model to ice flow and ablation parameters: Consequences for the evolution through the last climate cycle, *Clim. Dyn.*, *13*, 11–24.

Royer, D. L. (2006), CO_2-forced climate thresholds during the Phanerozoic, *Geochim. Cosmochim. Acta*, *70*, 5665–5675.

Thompson, S. L., and D. Pollard (1997), Greenland and Antarctic mass balances for present and doubled atmospheric CO_2 from GENESIS version-2 global climate model, *J. Clim.*, *10*(5), 871–900.

Veevers, J. J., and C. M. Powell (1987), Late Paleozoic glacial episodes in Gondwanaland reflected in transgressive-regressive depositional sequences in Euramerica, *Geol. Soc. Am. Bull.*, *98*, 75–487.

Veevers, J. J., P. J. Conaghan, C. M. Powell, E. J. Cowan, K. L. McDonnell, and S. E. Shaw (1994), Eastern Australia, in *Permian-Triassic Pangean Basins and Foldbelts Along the Panthalassan Margin of Gondwanaland*, edited by J. J. Veevers and C. M. Powell, *Mem. Geol. Soc. Am.*, *184*, 11–171.

Ziegler, A. M., M. L. Hulver, and D. B. Rowley (1997), Permian world topography and climate, in *Late Glacial and Postglacial Environmental Changes-Quaternary*, edited by I. P. Martini, pp. 111–146, Oxford Univ. Press, New York.

D. E. Horton and C. J. Poulsen, Department of Geological Sciences, University of Michigan, 2534 CC Little Building, Ann Arbor, MI 48109, USA. (danethan@umich.edu)

D. Pollard, Earth and Environment Science Institute, Pennsylvania State University, 2217 Earth-Engineering Sciences, University Park, PA 16802, USA.